EARTH SURFACE PROCESSES AND LANDFORMS
Earth Surf. Process. Landforms **35**, 319–330 (2010)

Published online 1 February 2010 in Wiley InterScience
(www.interscience.wiley.com) DOI: 10.1002/esp.1920

Tidal channel meander formation by depositional rather than erosional processes: examples from the prograding Skagit River Delta (Washington, USA)

W. Gregory Hood*
Skagit River System Cooperative, LaConner, WA, USA

Received 26 May 2009; Revised 9 August 2009; Accepted 10 August 2009

*Correspondence to: W. Gregory Hood, Skagit River System Cooperative, P.O. Box 368, LaConner, WA 98257-0368, USA. E-mail: ghood@skagitcoop.org

ESPL
Earth Surface Processes and Landforms

ABSTRACT: Channel meander dynamics in fluvial systems and many tidal systems result from erosion of concave banks coupled with sediment deposition on convex bars. However, geographic information system (GIS) analysis of historical aerial photographs of the Skagit Delta marshes provides examples of an alternative meander forming process in a rapidly prograding river delta: deposition-dominated tidal channel meander formation through a developmental sequence beginning with sandbar formation at the confluence of a blind tidal channel and delta distributary, proceeding to sandbar colonization and stabilization by marsh vegetation to form a marsh island opposite the blind tidal channel outlet, followed by narrowing of the gap between the island and mainland marsh, closure of one half of the gap to join the marsh island to the mainland, and formation of an approximately right-angle blind tidal channel meander bend in the remaining half of the gap. Topographic signatures analogous to fluvial meander scroll bars accompany these planform changes. Parallel sequences of marsh ridges and swales indicate locations of historical distributary shoreline levees adjacent to filled former island/mainland gaps. Additionally, the location of marsh islands within delta distributaries is not random; islands are disproportionately associated with blind tidal channel/distributary confluences. Furthermore, blind tidal channel outlet width is positively correlated with the size of the marsh island that forms at the outlet, and the time until island fusion with mainland marsh. These observations suggest confluence hydrodynamics favor sandbar/marsh island development. The transition from confluence sandbar to tidal channel meander can take as little as 10 years, but more typically occurs over several decades. This depositional blind tidal channel meander formation process is part of a larger scale systemic depositional process of delta progradation that includes distributary elongation, gradient reduction, flow-switching, shoaling, and narrowing. Copyright © 2010 John Wiley & Sons, Ltd.

KEYWORDS: tidal channel meander; channel bar; channel confluences; delta progradation; river distributary

Introduction

Tidal channels are commonly considered to originate from tidal erosion of intertidal plains (Allen, 2000; Fagherazzi and Sun, 2004; D'Alpaos *et al.*, 2005). At a smaller scale, channel meander bends are likewise considered the result of sediment transport processes in which erosion is prominent (Leopold *et al.*, 1964; Knighton, 1984; Eisma, 1998; Solari *et al.*, 2002; Fagherazzi *et al.* 2004). Erosion carves the concave side of a channel meander, while sediments deposit on the convex side, forming or extending a point bar. However, the universality of the erosional paradigm of tidal channel formation has been challenged by observations of depositional channel network development in prograding deltas (Hood, 2006; Kirwan and Murray, 2007).

The first objective of this paper is to show that depositional processes in a prograding river delta act consistently at several scales to form particular tidal channel meanders in addition to tidal channel networks. Depositional meander formation in the Skagit Delta (Washington, USA) will be shown to proceed from sandbar development in a river distributary near the outlet of a tributary blind tidal channel. Further sandbar growth leads to colonization and stabilization by vegetation and thus formation of a marsh island. The gap between the new marsh island and the mainland marsh eventually narrows to close on one side of the blind channel outlet, thereby joining the island to the mainland; the gap remains open on the other side of the outlet (due to tidal prism available to the blind tidal channel), thereby forming a meander bend and extension of the blind tidal channel (Figure 1). Evidence for this distinctive pattern of depositional tidal meander bend formation comes from direct observation of channel planform evolution in chronosequences of historical aerial photographs. The historical channel planforms are shown to coincide with

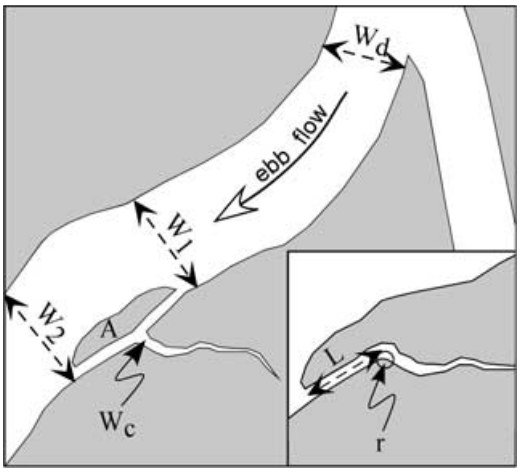

Figure 1. Definition sketch. The main figure shows a historical planform, when a marsh island is located at the mouth of a blind tidal channel. The insert shows the modern planform following island junction to the mainland with consequent meander formation. L = straight-line length from historical (pre-meander) channel outlet to current (post-meander) channel outlet; W_c = width of historical channel outlet; A = area of meander-forming island; W_d = distributary width below a distributary bifurcation point; W_1 and W_2 = distributary widths just upstream and downstream of the meander-forming island respectively; r = radius of meander bend curvature.

current marsh topographic legacies, which are interpreted as relict shorelines, analogous to meander scroll bars. The second objective is to investigate whether the marsh islands that form within river delta distributaries are randomly distributed and only incidentally block blind tidal channel tributaries, or whether the islands are positively associated with blind tidal channel tributary outlets, perhaps as a consequence of tributary-distributary junction hydrodynamics. The third objective is to explore possible predictors of the rate of meander formation, with the expectation that large blind tidal channel tributaries would form meanders more slowly than small ones because their greater tidal prism could retard island-mainland fusion.

Distinguishing systems in which depositional versus erosional channel-forming processes predominate may provide useful guidance for further refinement of morphodynamic models, and for land-use management affecting sediment supply or river discharge to deltaic systems. A more complete paradigm of tidal channel formation that includes deposition-dominated as well as erosion-dominated variants will also provide greater insight into tidal marsh restoration. For example, crevasse splay-mediated marsh restoration projects in the Mississippi River Delta (Coleman, 1988; Boyer *et al.*, 1997; Day *et al.*, 2007) will likely be characterized by depositional channel formation.

Setting

The study area is located in the tidal marsh of the South Fork Skagit River Delta (Figure 2). The river drains 8544 km^2 of the Cascade Mountains, with elevations reaching 3285 m. Mean annual rainfall ranges from 80 cm in the lowlands to over 460 cm in the mountains. River flow peaks in winter (storm runoff) and again in late spring (snow melt), with low flows in September. Mean discharge at Mount Vernon is 468 m^3 s^{-1} with maximum and minimum recorded flows of 5100 and 78 m^3 s^{-1}, respectively (Wiggins *et al.*, 1997). The Skagit is the largest river flowing into Puget Sound, providing 34–50% of the Sound's freshwater and sediment inputs, depending on the season (Babson *et al.*, 2006). The river provides a comparable contribution to regional production of wild Pacific salmon (*Oncorhynchus* spp.), a culturally and economically important resource dependent on tidal marshes and channels for rearing habitat (Reimers, 1971; Nickelson and Johnson, 1991; Magnusson and Hilborn, 2003); juvenile wild Puget Sound Chinook salmon are most dependent on tidal channel habitat and are a threatened species (US Federal Register, 1999). This habitat is also important to other fish and wildlife, ranging from commercially important Dungeness crab (*Cancer magister*) to marine mammals (Simenstad, 1983). Due to the ecological significance of tidal marshes and their channels, considerable effort and resources are being directed by local, state, and federal agencies towards estuarine habitat restoration in Puget Sound, as well as many other regions. Effective management requires understanding the natural processes that form and maintain habitat in a dynamic landscape.

Significant anthropogenic changes in the delta began with Euro-American settlement in the 1860s. By 1890, dikes and levees had been constructed to allow farmland development. The delta is now bordered by only a narrow fringe of tidal marsh (<0·5 km wide), with significant remnant marsh only near the North and South Fork outlets. At 12 km^2, the South Fork marshes are three times as extensive as the North Fork marshes. Upriver anthropogenic changes include logging, bank hardening, and dam construction on the Skagit River and a tributary, the Baker River. The dams intercept water and sediment flows from about 47% of the Skagit basin. The largest Skagit River tributary, the Sauk River, is still undammed and drains 23% of the basin.

Marsh sediments are principally organic-rich silt, silty clay and fine sand, while unvegetated tidal flats are fine to medium sand. Marsh vegetation (from low to high elevation) consists primarily of *Schoenoplectus americanus* (American three-square), *Carex lyngbyei* (sedge), *S. tabernaemontani* (soft-stem bulrush), *Typha angustifolia* (cattail), *Myrica gale* (sweetgale), *Salix* spp. (willow), and *Picea sitchensis* (Sitka spruce). During spring tides the tidal range approaches 4 m and the marsh can be inundated by up to 1·5 m of water. Tides in Skagit Bay are mixed, semi-diurnal dominant tides and show large inequalities in tidal range and strong spring-neap tidal cycle; for more details on Skagit Bay hydrodyanamics see Yang and Khangaonkar (2009).

Methods

GIS analysis

A geographic information system (GIS) was used to compare true color (2007, 2000) and infrared (2004) digital orthophotos, black and white historical aerial photographs (1937, 1956, 1964, 1965, 1972, 1991, 1998), and infrared historical aerial photographs (1971, 1981, 1984, 1987, 1990, 1994, 1996). The 2007 true color orthophotos had 30-cm pixels, were 1 : 12 000 scale, and flown April 3 during mid tide (+2 m MLLW) when large sandbars and higher sandflats were exposed. Channels as small as 60 cm wide were distinguishable in the 2007 photographs because marsh vegetation was either ankle-high or sparse at this time of year. Historical photographs were scanned at 800 dpi resolution. The 1964 photographs had 60-cm pixels, were 1 : 20 000 scale, flown August 24 at a minus tide that exposed sandflats in the bay; the smallest distinguishable channels were 1·2 m wide. The 1971 (October 16) and 1981 (August 8) photographs had

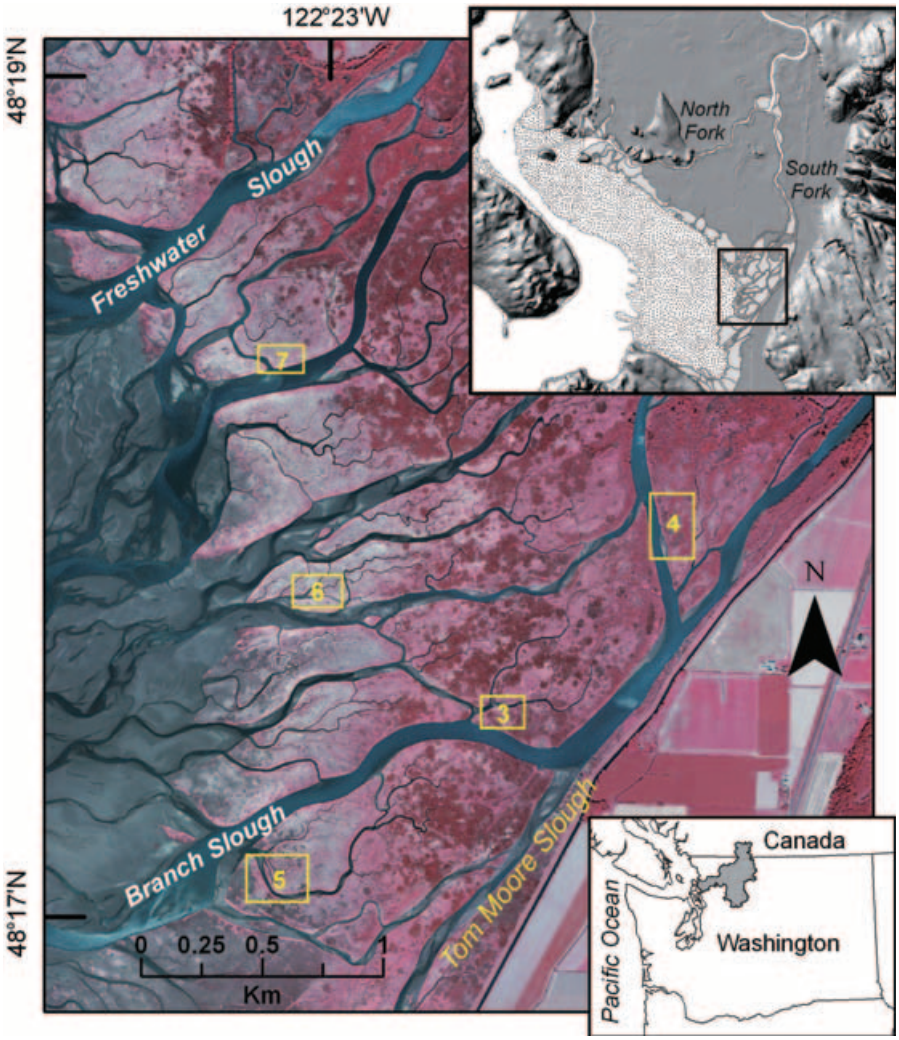

Figure 2. Location map of five examples of depositional meander development detailed in Figures 3–7; labeled boxes are scaled approximately to the frames in the three figures. The photograph is from 2004. The top inset shows the active Skagit Delta with a black square showing the spatial extent of the main figure. Stippled areas in the inset are the sandy tide flats of Skagit Bay. Light grey areas landward of the flats are vegetated tidal marshes; dark grey areas are predominantly farmed lowlands. This figure is available in colour online at www.interscience.wiley.com/journal/espl

2·5-m and 2·0-m pixels, respectively, were 1 : 58 000 scale, flown at mid tide when sandbars were obscured; the smallest distinguishable marsh channels were 3·5 m and 3·0 m wide, respectively. The 1984–1996 photographs were flown by the US Army Corps of Engineers at 1 : 12 000 scale during summer. Pixel size was 3·3 m for 1984 and 1·3 m for other years. The narrowest observable channel was 4 m wide for 1984 and 2 m wide for the others. Sandbars were exposed for the 1987, 1994, and 1996 photographs. The 1998 photograph had 0·9 m pixels, was at 1 : 60 000 scale, with partially exposed sandbars, and minimum observable channels 1·5 m wide. Details on the other aerial photographs have been reported previously (Hood, 2006). A georeferenced 1889 US Coast and Geodetic T-sheet of the Skagit Delta (Puget Sound River History Project, University of Washington) allowed only approximate location of historical shorelines due to low resolution.

All historical photographs were rectified relative to the 2000 orthophotos using reference points (e.g. road intersections) visible in both historical and recent photographs. For all photographs, tidal channel margins and other shorelines were manually digitized in the GIS. Shorelines were defined by the abrupt transition from vegetated to unvegetated intertidal areas. Distinct photograph signatures almost always allowed vegetated and unvegetated areas to be clearly distinguished. Ambiguous exceptions were not analyzed. Further details of the photograph analysis, including estimation of rectification and digitization error have been previously described (Hood, 2004, 2006).

Planform data collected from aerial photographs (Figure 1) included (1) width (W_c) of a historical blind channel outlet prior to meander bend formation; (2) length (L) of the additional channel resulting from meander formation; (3) surface area (A) of the island blocking the historical blind channel outlet and forming the meander, measured just prior to island junction with the mainland marsh; (4) upstream width (W_d) of the distributary delivering sediment to form sandbars and marsh islands – the upstream width was located just below a distributary bifurcation and was generally the narrowest part of the distributary; (5) the average of the distributary widths just upstream (W_1) and downstream (W_2) of the meander-forming island; (6) island distance upstream from a distributary's bay outlet; (7) the span of years in the available photographs during which an unvegetated sandbar was present at the mouth of the historical blind channel prior to meander formation; (8) the span of years during which a veg-

etated marsh island was present at the mouth of the historical blind channel; (9) radius of meander curvature (r), estimated by manually fitting circles to the meander in the GIS.

Seventeen separate year-sets of historical aerial photographs were available to illustrate the chronology of meander formation. While all year-sets were evaluated in GIS for change analysis, only year-sets marking significant morphological transitions are depicted in accompanying figures so that graphical clarity and interpretability could be maximized.

Scaling of meander length versus channel width was investigated for blind tidal channels whose meanders were apparently formed depositionally, forced by marsh island formation at an historical channel outlet. Channels in the 2007 aerial photographs were selected for analysis according to two criteria: (1) historical aerial photographs documented depositional meander formation through marsh island forcing; or (2) channel planform and topography were strongly consistent with those associated with depositional meander formation observed in photographic chronosequences. The diagnostic value of channel planform and topography are detailed in the results and discussion. Topographic breaks were interpreted in the 2007 aerial photographs from easily observed and distinct patterns in the vegetation. In upstream portions of the delta, historical river levees are frequently occupied by shrubs, with cattails and sedges at lower elevation; in lower portions of the delta cattails often occupy historical levees with sedges at lower elevation (Hood, 2007a). Meanders were delimited by the apex of the first and third channel bends in a series. Cartesian meander length (L_x) was the straightline distance from one end of the meander to the other; intrinsic meander length (L_s) was the along-channel length of the meander (Marani *et al.*, 2002). Of the 12 meanders investigated, nine satisfied the photographic criterion, while the remainder relied on planform and topographic evidence for inclusion. Mean channel width was defined, using GIS, as the surface area of the meander segment divided by L_s. The value of L_s was one-half of the perimeter of the meander segment minus its upstream and downstream widths.

Topography

Marsh topography was modeled in a GIS from LiDAR data collected during a spring low tide in April 2002 at an average spacing of 3 m with horizontal accuracy of 20 cm and vertical accuracy of 15 cm. Ground-truthing through global positioning surveying (GPS; 2 cm horizontal and vertical resolution) revealed that, in spite of post-processing to determine 'bare-earth' elevation, LiDAR was most accurate in areas vegetated with ankle-high early season sedge, less so in areas of cattail, and very inaccurate in shrubby areas (Hood, 2007b). Consequently, elevation was modeled only for areas where sedge predominated and shrubs were absent. In areas with abundant shrubs, relative surface elevation was measured with a laser level (CST/berger LMH-C; accuracy of ±2·4 mm at 30 m) along survey transects. Transects were perpendicular to shorelines and delineated with a measuring tape. GPS (50 cm resolution) mapped transect end points and intersected channel banks so that GIS could spatially relate the modern survey data to channel features in historical aerial photographs.

Statistical analysis

Stepwise linear regression (SYSTAT 10.2, Systat Software, Inc., Point Richmond, CA, USA) evaluated the ability of log-transformed planform morphological variables (described earlier) to predict rates at which vegetated marsh islands fused with mainland marsh to form channel meander bends, and island size just prior to fusion. Similar analysis to predict rates of sandbar development into vegetated marsh islands was not possible because several historical photographs were flown during relatively high tides, preventing sandbar observation. This critically reduced the sample size available for sandbar analysis.

A 2 × 2 chi-square contingency analysis (Zar, 1999) evaluated whether islands were located randomly within river distributaries or if they were associated with tributary tidal channel outlets. Distributaries were divided into 100-m segments starting from their outlets. Each bank segment was classified as 'island present' versus 'island absent' and 'tributary outlet present' versus 'absent'. Islands were associated with the nearest bank. Where outlet-associated islands spanned more than one river segment, an uncommon event, each segment was classified as containing an island and a tributary outlet. Data were collected for all distributary islands throughout the historical period covered by the aerial photographs. Individual islands were only counted once during their history. The criterion for statistical significance was $p < 0{\cdot}05$ for all analyses.

Results

Chronosequences

Seventeen cases of depositional blind tidal channel meander formation involving at least one channel bend (half-meander) were observed during GIS change analysis of historical aerial photographs of the South Fork Skagit Delta; gaps in the photographic record likely prevented observation of more cases. For the sake of brevity, five representative examples of depositional blind tidal channel meander formation are discussed. The first example (Figure 3) is located near the downstream end of a very minor river distributary that was as narrow as 8 m at its upstream end in 1956 and 1972, but today is less than 2 m wide. Downstream, the distributary was 24–30 m wide in 1956, becoming more uniformly 24 m wide in 1972, while today it is only 14–18 m wide. Near the tributary blind tidal channel, the mainland marsh shoreline was relatively stable from 1937 to 1990, and transects A_1 and A_2 show a berm just landward of this shoreline. In A_1 the berm is 8 m wide and 10 cm higher than the marsh plain behind it. In A_2 the berm is 9 m wide and up to 18 cm higher than its hinterlands. By 1981 a large vegetated island developed with a 2·5 m gap between it and the mainland; by 1990 the island had lengthened downstream. The eastern (upstream) half of the 1990 island/mainland gap aligns perfectly with the eastward bend of the modern blind tidal channel that formerly emptied into the gap midsection. By 1998 the western half of the gap filled in to now coincide with the deepest part of a 6-m wide and 15-cm deep vegetated swale in transect A_1. An additional berm is found on transect A_1 behind the current shoreline, which was relatively stable from 1990 to 2007. On transect A_2, a large berm is present where the shoreline was stable from 1990 to 2000, while topographic breaks seaward of the berm correspond to prograding 2004 and 2007 shorelines. Well landward of the 1937 shoreline, a third berm was found on transect A_2 just landward of a small 1-m wide and 30-cm deep channel (labeled T_3 in Figure 3) found in the field survey and in the 1937 photograph, but not in any subsequent photographs. This berm likely marks a marsh shoreline formed

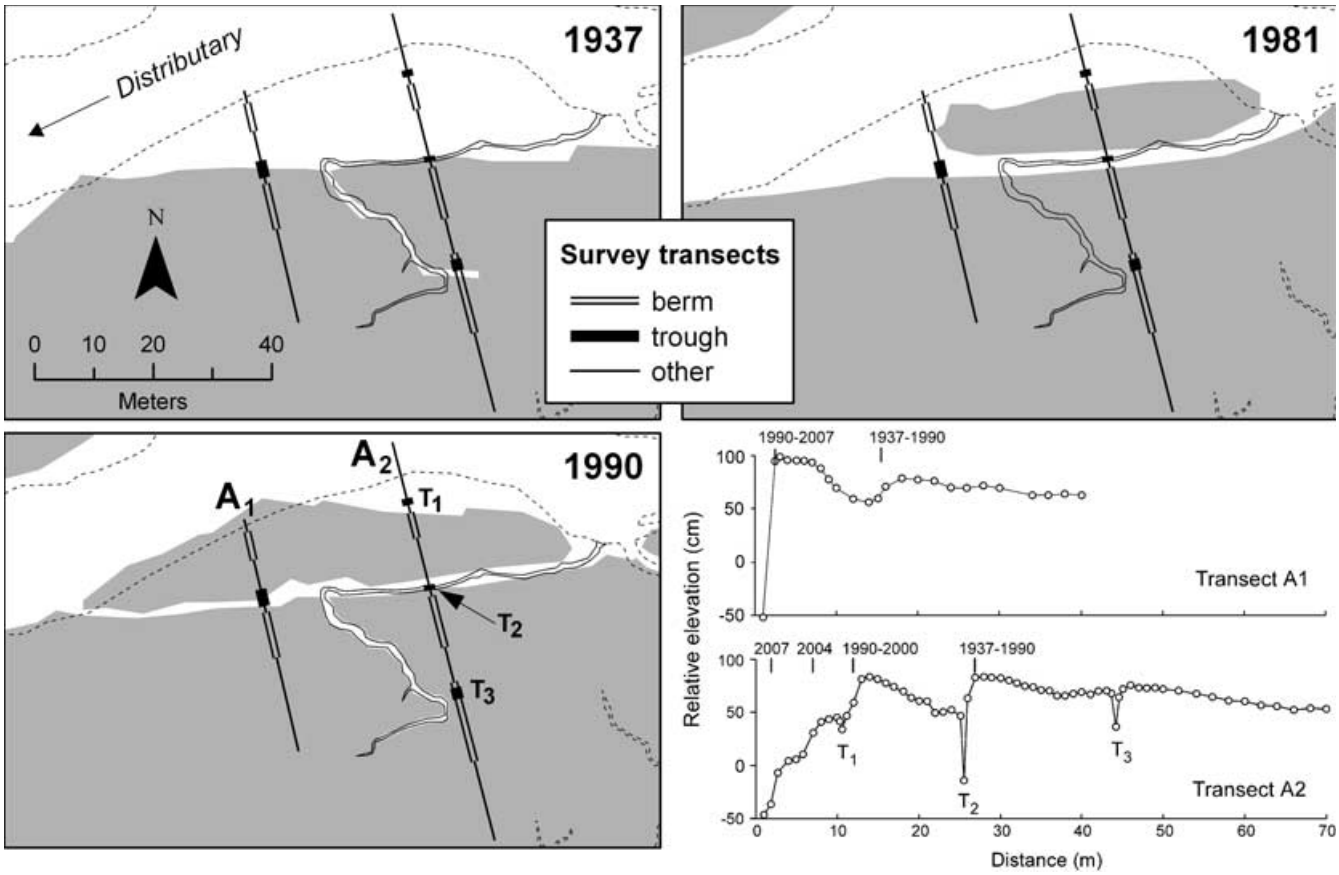

Figure 3. Depositional meander development from 1937 to 1981 (when a vegetated island formed near a blind tidal channel outlet) to 1990 (just prior to island junction with the mainland). The 2007 channel of interest (solid outline) is superimposed on all figures. Dashed lines are marsh boundaries in 2007. Many non-essential photo-years are omitted for graphic economy. Arrow indicates direction of dominant distributary flow. Marsh topography was surveyed along transects A_1 and A_2. Berms are marked by open bars along the transect. Intersected channels and swales, i.e. transect troughs, are marked by solid bars. Multiple troughs in a transect are labeled T_n in order from the shoreline. Transect profiles (lower right frame) begin in the distributary channel. Elevations are relative, with the lowest marsh plain arbitrarily set at 50 cm. Locations of historical shorelines observed in aerial photographs are denoted by labeled short vertical bars above each profile.

between 1889 and 1937 and stable for several decades during this interval.

The second example (Figure 4) is located in the second largest of the South Fork Skagit River distributaries. There are two tributary blind tidal channel systems here and the distributary is currently 40–50 m wide in this area. A large marsh island formed at the mouth of the more northerly blind tidal channel between 1964, when only a large sand bar was present, and 1972. By 1990 the island was completely incorporated into the mainland with no additional changes from 1990 to the present. The 4- to 16-m-wide gap between the 1972 island and mainland was from 1990 to 2007 a 1·5- to 3·5-m-wide 70° downstream extension of the blind tidal channel. The island extended northwards (upstream) between 1972 and 1990 to connect with the mainland. In so doing, it diverted a smaller neighboring tidal channel in the downstream direction in a manner similar to that just described, so that this previously independent blind channel became a tributary to its neighbor by 1990. The course of the new tributary junction lies between the 1972 mainland and a northwards extension of the 1972 island. The B_1 and B_2 topographic transects reveal sizeable berms near the 1990–2007 shorelines, both 40–50 cm higher than the marsh plain. Smaller berms are located near the 1937 shoreline on both transects. On B_1, this berm is 5–8 cm above the marsh plain and preceded seaward by a 22-cm deep and 2-m wide swale. On B_2, the berm is 10 cm high and preceded by an 8-cm deep and 2-m wide swale. There is also a small 5-cm high berm near the 1956–1972 shorelines on B_1, which is preceded seaward by a 14-cm deep and 5-m wide swale. Being paired with a seaward swale and historical shorelines visible in aerial photographs distinguishes these berms from an apparently random topographic irregularity. The adjacent, downstream blind tidal channel system has not experienced significant planform changes during the historical period. However, a sandbar was present at the mouth of this channel system from 1964 to 1998, which then developed into increasingly numerous and large vegetated marsh islands from 2000 to 2007 (Figure 4). Assuming continuation of their historical trajectory from sandbar to vegetated islands, these islands appear likely to coalesce in the next decades and force an approximately right-angle meander in this adjacent blind tidal channel system.

The third example (Figure 5), is located in a minor distributary, only 7 m wide near its upstream end from 1937 to the present. Between 1937 and 1956 a marsh island developed near the downstream end of the distributary, at the outlet of a large tributary blind tidal channel system (1956 outlet width = 6 m). The island became increasingly larger in the 1972 and 1990 aerial photographs. Island growth coincided with westward displacement of the western distributary bank, which eroded 3–4 m from 1937 to 1956 and 6–7 m from 1956 to 1972. No further erosion occurred from 1990 to the present. The eastern distributary bank was unchanged from 1937 to 1991. The northern (downstream) half of the marsh

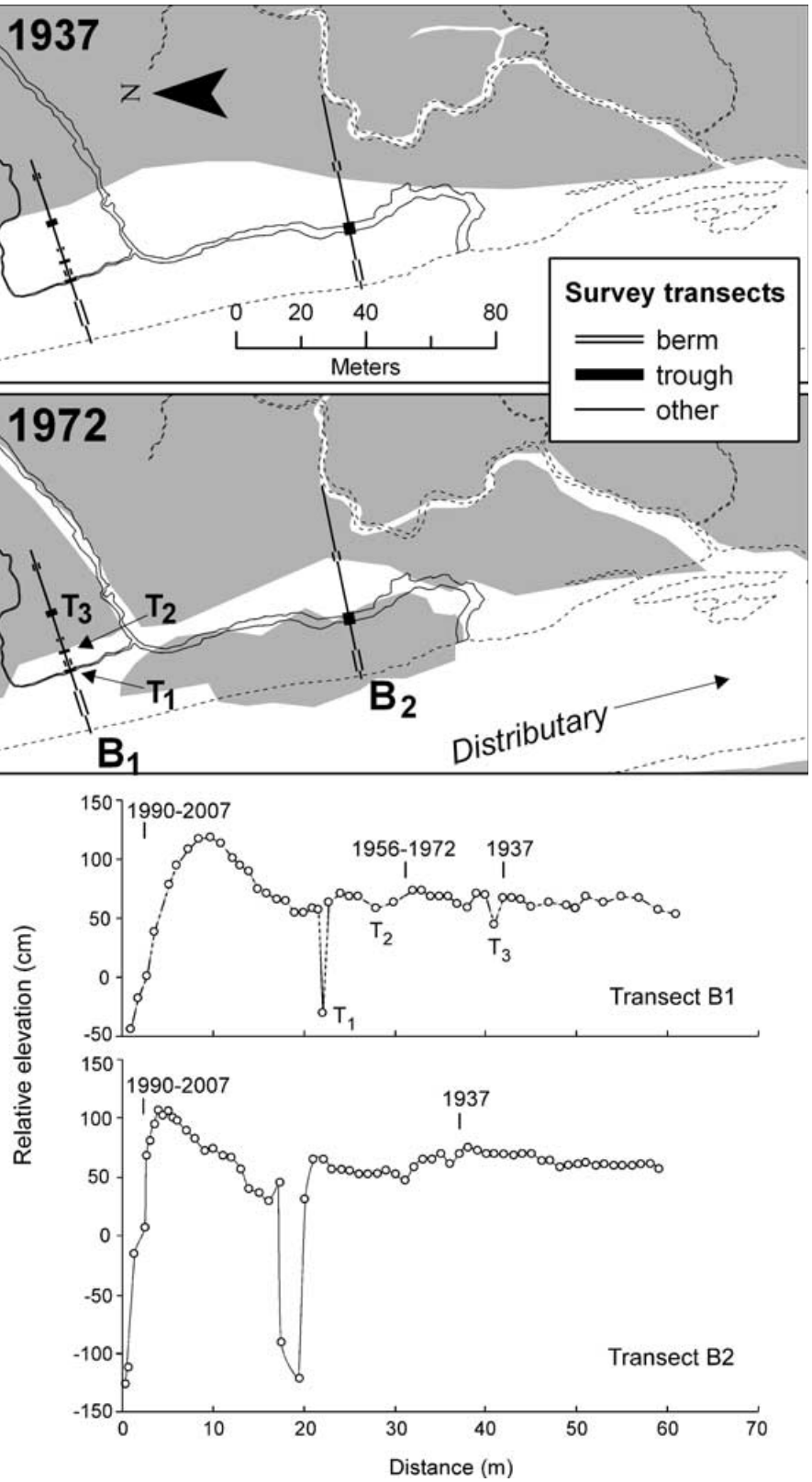

Figure 4. Depositional meander development from 1937 to 1972 (when a vegetated island formed near a blind tidal channel outlet). The 2007 channel of interest (solid outline) is superimposed on all figures. Dashed lines are marsh boundaries in 2007. Many non-essential photo-years are omitted for graphic economy. Arrow indicates direction of dominant distributary flow. Marsh topography was surveyed along transects B_1 and B_2. Berms are marked by open bars along the transect. Intersected channels and swales, i.e. transect troughs, are marked by solid bars. Multiple troughs in a transect are labeled T_n in order from the shoreline. Transect profiles (bottom frame) begin in the distributary channel. Elevations are relative, with the lowest marsh plain arbitrarily set at 50 cm. Locations of historical shorelines observed in aerial photographs are denoted by labeled short vertical bars above each profile.

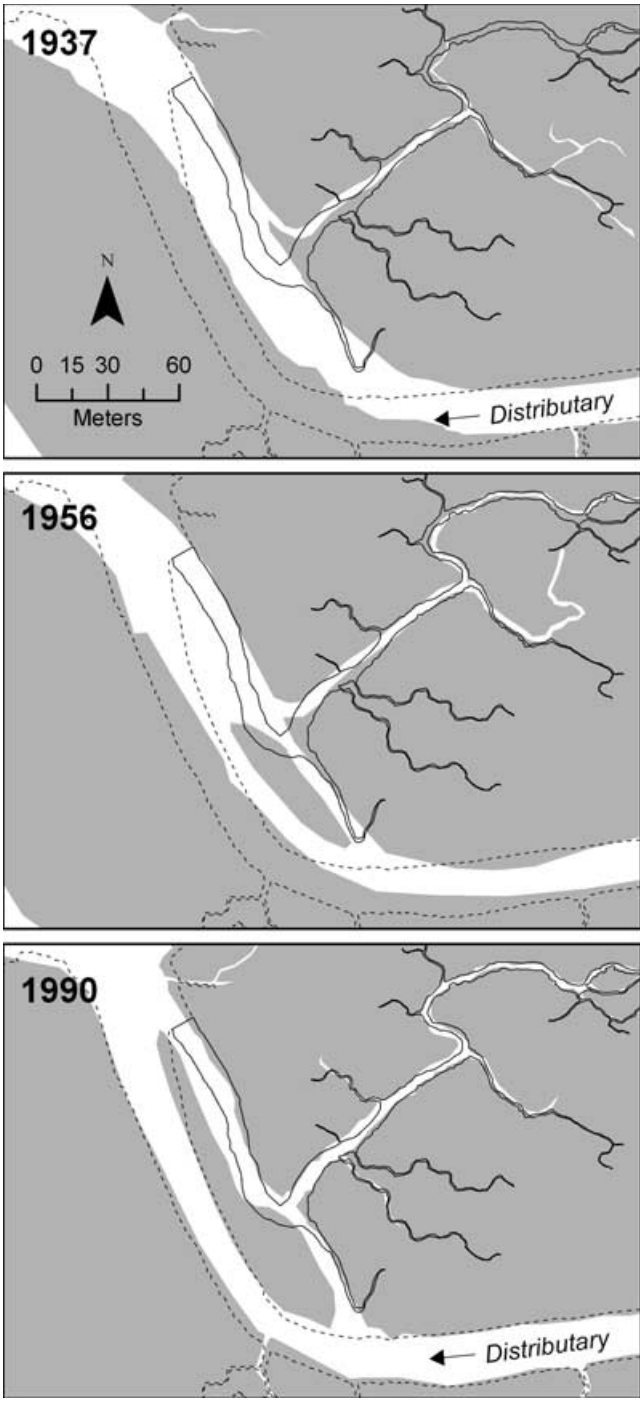

Figure 5. Depositional meander development from 1937 to 1956 (when a vegetated island formed near a blind tidal channel outlet) to 1990 (when the island elongated downstream). The 2007 channel of interest (solid outline) is superimposed on all figures. Dashed lines are marsh boundaries in 2007. Many non-essential photo-years are omitted for graphic economy. Arrow indicates direction of dominant distributary flow.

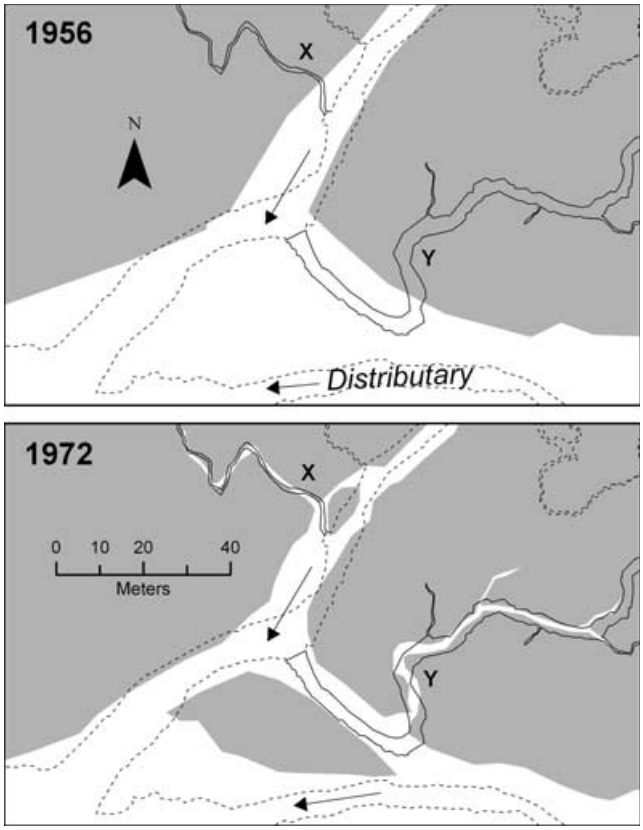

Figure 6. Depositional meander development from 1956 to 1972 (when vegetated islands formed near two blind tidal channel outlets, X and Y). The 2007 channels of interest (solid outlines) are superimposed on all figures. Dashed lines are marsh boundaries in 2007. Many non-essential photo-years are omitted for graphic economy. Arrows indicates direction of dominant distributary flow.

island/mainland gap narrowed from about 12 m in 1990 to 8 m by 2007 to become a right angle seaward extension of the trunk of the blind channel system. Meanwhile, the southern (upstream) half of the marsh island/mainland gap narrowed from 7 m in 1990 to 3 m in 1991. By 2000 this portion of the gap was completely obstructed at its extreme upstream end, but did not fill in entirely. Instead, it formed a new 2-m wide tributary to the original blind tidal channel system by capturing an adjacent small pre-existing tidal channel that drained the marsh into the this portion of the island/mainland gap. As in this case, gap narrowing can form a new tributary if sufficient tidal prism from captured channels and adjacent marsh is available to keep it open. Otherwise, the gap fills and becomes a vegetated swale.

The next example (Figure 6) illustrates that this depositional, island-mediated, meander formation process can generate both large (140°) and relatively small (60°) meander bends, and that even small islands can cause meander development. Marsh islands formed near the mouths of blind channels X and Y between 1956 and 1972. Channel X was 1·6 m wide in 1972 and debouched near a 55-m^2 island; channel Y was 6·0 m wide and debouched near a 660-m^2 island. By 1990 the upstream ends of the island/mainland gaps became obstructed so that both blind channels developed meander bends that extended downstream within the remaining unobstructed portion of the gaps. From 1990 to 2007 there were no significant changes in channel planform.

The last example (Figure 7) includes LiDAR-derived topography and further illustrates how island formation pairs meander bend development with a topographic legacy. In this case a small island developed at a blind tidal channel outlet in 1964 with consequent channel redirection to the east by 1990. By 1990 additional islands formed, extending the blind tidal channel and confining it to the edge of the 1937–1964 mainland shoreline. Topographic highpoints outlined by elevation contours tend to coincide with the 1964 and 1990 island locations, particularly those most seaward of the historical mainland shorelines.

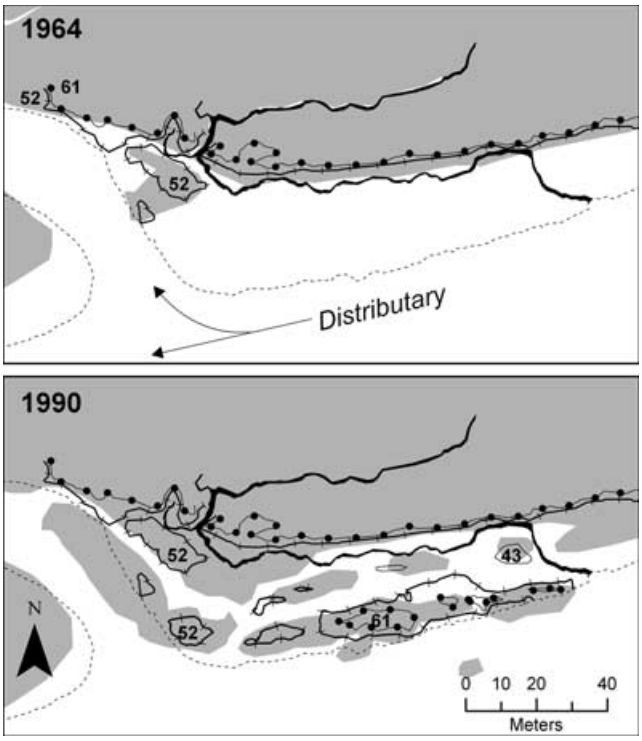

Figure 7. Depositional meander development in 1964 and 1990 when marsh islands formed near the mouth of a blind tidal channel outlet. The 2007 channel of interest (solid black) is superimposed on all figures. Dashed lines are marsh boundaries in 2007. Many non-essential photo-years are omitted for graphic economy. Arrows indicates direction of dominant distributary flow. Contour lines (in centimeters, NGVD 1929) derived from GIS analysis of 2002 LiDAR data are shown as they relate to each historical image. Ball-pattern, hatched, and plain contours represent the 61-, 52-, and 43-cm contours, respectively. For graphic clarity, only contours of high points seaward of the 1964 shoreline are shown.

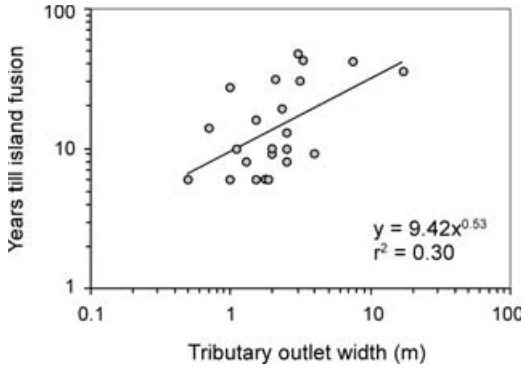

Figure 8. Rate of island fusion with marsh mainland to form blind channel meander bends, predicted by the width of the blind channel outlet prior to island fusion.

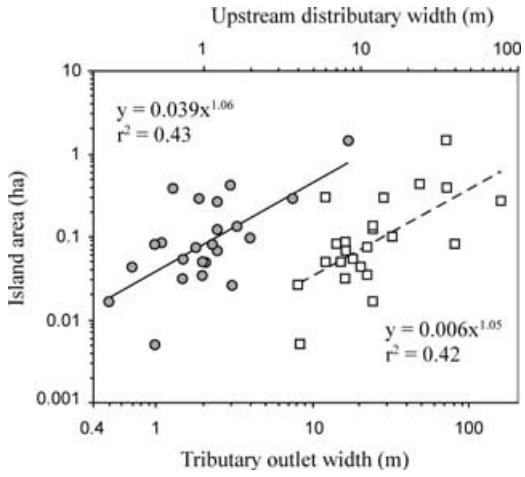

Figure 9. Size of meander-forming islands relative to upstream distributary width (open squares) or the width of tributary blind channel outlets which the islands obstruct (filled circles).

Process rate

Marsh islands persisted an average of 18 years [n = 22, maximum = 47 years, minimum = 6 years, standard deviation (SD) = 13·9 years] from first observation in an aerial photograph to first observation of their junction with an historical marsh mainland and the formation of a meander bend. Precursor sandbars persisted an average of 14·6 years (n = 9, maximum = 27 years, minimum = 4 years, SD = 8·3 years) from their first observation in an aerial photograph to their conversion to a vegetated marsh island. The sandbar results must be considered with caution because of small sample size and because several historical aerial photographs were flown at tides covering sandbars. Nevertheless, the minimum observed time interval between sandbar or vegetated island formation and conversion should be relatively reliable. These minimum intervals indicate depositional meander development can take as little as 10 years from initial sandbar development to meander bend formation. Step-wise regression indicates only tributary blind channel outlet width has predictive power for meander formation rate; the wider the outlet, the longer the time for island fusion and meander formation (Figure 8; R^2 = 0·30, p < 0·01). Relative to small blind tidal channels, the greater tidal prism of large channels is more capable of flushing both forks of the island/mainland gap and retarding island fusion with the mainland.

Island distribution and geometry

There are currently 35 islands or island clusters located within river distributaries of the South Fork Delta, of which 83% are associated with the mouths of blind tidal channels tributary to a distributary. If historical islands are included for consideration, 72% of all observed islands or island clusters have been associated with tributary blind tidal channel outlets. A 2 × 2 contingency analysis indicates significant association between islands and tributary channel outlets (chi-square = 28·29, p < 0·0001).

Stepwise regression indicates tributary outlet width (W_c) and upstream distributary width (W_d) are the best available predictors of the area (A) of meander-forming islands ($\log A = -2{\cdot}244 + 0{\cdot}849 \log W_c + 0{\cdot}836 \log W_d$; R^2 = 0·67, p < 0·0001). Both predictors account approximately equally for variation in island area, and both independently account for about 42% of island size variation (Figure 9). There is no significant correlation between the predictors (r = 0·24). As might be expected, the length of new blind tidal channel, forced by meander-forming marsh islands at blind tidal channel confluences with river distributaries, scales isometrically with island length, i.e. with an exponent indistinguishable from one (Figure 10). Scaling of island length and area with new channel length and outlet width, respectively, suggests meander length could scale with channel width. This is the case for Cartesian

(L_x; Figure 11) and intrinsic (L_s; not shown) meander length. Furthermore, length–width scaling of Skagit Delta blind tidal channel meanders formed by deposition-dominated processes is comparable to that for purely fluvial and purely tidal systems where meanders are formed by erosion-dominated processes. Skagit tidal meander sinuosity (L_s/L_x) averages 1·5 (range 1·1 to 2·7) and is likewise comparable to fluvial meanders (Williams, 1986; Marani *et al.*, 2002).

Discussion

Marani *et al.* (2002) state that, '. . . when the physical mechanisms governing the spatial development of meanders act at a scale comparable with their width, the landforms generated exhibit strong similarities independently of the nature of the processes that shape them.' Consistent with this principle, the size of meander-forcing marsh islands in the Skagit Delta scales with blind tidal channel outlet width; likewise the lengths of island-forced meanders scale with channel width similarly to a wide variety of fluvial and tidal systems (Figure 11). Consequently, the depositional tidal channel meander formation process seen in the rapidly prograding Skagit Delta is a true meander forming process, not merely a process that forms haphazard channel bends.

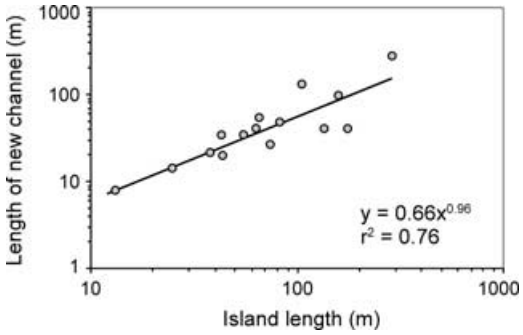

Figure 10. The length of new blind tidal channel meander forced by marsh island formation and fusion with the mainland at a blind tidal channel and river distributary confluence, versus the length of the island.

In purely tide-dominant systems, blind tidal channel meanders result from coupled sediment erosion and deposition driven by tidal energy and focused, respectively, in the concave and convex portions of a channel bend (Fenies and Faugères, 1998; Marani *et al.*, 2002; Solari *et al.*, 2002; Fagherazzi *et al.*, 2004; McClennen and Housley, 2006). The bar theory of river meandering (Blondeaux and Seminara, 1985; Solari *et al.*, 2002) proposes that alternate bars force bank erosion and thereby trigger meander development. In contrast, examples from the river-dominated Skagit Delta illustrate a meander formation process in blind tidal channels that is predominantly depositional and that is occurring concurrently with significant delta progradation and distributary elongation, switching, and senescence; distributary senescence is characterized by channel infilling and eventual abandonment (Hood, 2004, 2006, 2007b). In this case, junctions of tributary blind tidal channels with senescing and narrowing river distributaries trigger the formation of bars at the tributary mouth which evolve into marsh islands and force the formation of a tributary meander.

In the South Fork Skagit Delta, most distributaries have been narrowing since at least 1956 (Hood, 2004). This has occurred in large part through marsh island development within distributaries, followed by island fusion with mainland marsh. Distributary senescence has been particularly notable in Tom Moore Slough (Figure 2), a late nineteenth-early twentieth century shipping channel, which has narrowed by half of its historical width and clearly shoaled throughout the historical aerial photograph series; navigation is now only possible by small boats, canoes, and kayaks at high tide. Marsh island development has likewise been most common within this

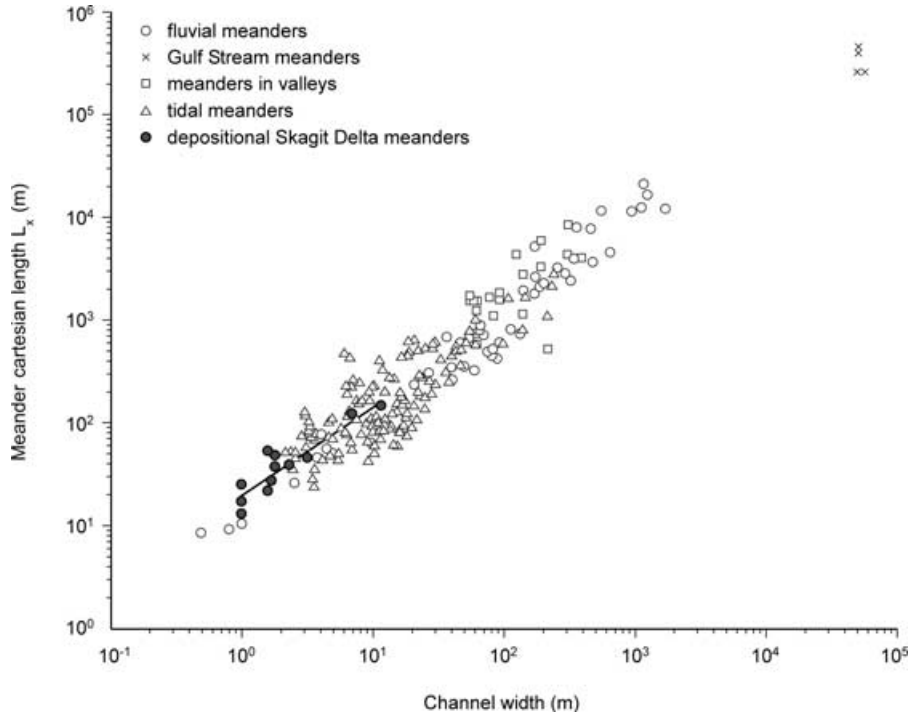

Figure 11. Cartesian meander length versus channel width for Skagit Delta blind tidal channel meanders forced by marsh island formation at blind tidal channel and river distributary confluences (filled circles; $y = 20x^{0.86}$, $R^2 = 0{\cdot}84$). Fluvial (open circles), Gulf Stream (crosses), fluvial valley (open squares), and tidal (open triangles) meanders are shown for comparison and are adapted from Marani *et al.* (2002).

distributary. In contrast, only two of 12 South Fork distributaries have widened since 1956. Branch Slough has widened to accommodate flows diverted from its senescing bifurcation partner, Tom Moore Slough. The erosional state of Branch Slough has made it the only major river distributary in which island formation was consistently absent throughout the historical record. Freshwater Slough has also widened to become the principal South Fork distributary. However, while the course of Branch Slough has been relatively static, Freshwater Slough meanders have migrated, possibly influenced by adjacent dikes constructed in 1960 (Hood, 2004). This migration has resulted in island formation near point bars of new distributary meanders. Nevertheless, island formation has been less common in Freshwater Slough than in senescing distributaries.

Marsh islands are not randomly distributed along senescing distributaries, but are instead associated with tributary blind tidal channel outlets. River distributary sandbars located near tributary blind tidal channel junctions tend to accumulate sediment and evolve into marsh islands. The gap between an island and the marsh mainland fills with additional sediment, resulting in fusion of the island and mainland along much of the gap, and a meander bend and downstream elongation of the tributary blind tidal channel along the remainder of the former island-mainland gap. This depositional meander formation process in blind tidal channels is recognizable from diagnostic signatures in channel planform and marsh topography. A sequence of several nearly right-angle tributary meander bends alternating with shore-parallel channel reaches suggests sequential formation of tributary-blocking and meander-forming marsh islands during distributary narrowing. This signature is strengthened with the concomitant observation of parallel sequences of marsh ridges and swales that are historical distributary levees adjacent to filled former island/mainland gaps, and are analogous to meander scroll bars in fluvial systems.

Tributary blind tidal channel outlet width (and consequently tributary size) is positively correlated with the size of the marsh island that forms at the outlet, and the time until island fusion with mainland marsh. This, along with the positive association between marsh islands and tributary outlets, suggests the hydrodynamics of distributary and tributary blind tidal channel confluences creates depositional zones near tributary outlets and influences confluence morphodynamics. The hydrodynamics of tidal distributary-blind tributary junctions remain to be explained in more detail. For example, what determines the direction in which a channel meanders – which half of the island/mainland gap is fated to close and which becomes a channel? Some new channels turn upstream, others downstream. Most bar-forming sediment presumably comes from the river, but how does flood-tide redistribution of sediment influence bar dynamics?

Channel confluences observed in the prograding Skagit Delta differ from confluences described for purely fluvial or purely tidal systems. In fluvial systems, symmetrical channel confluences with identical water and sediment discharge develop a symmetrical mid-channel bar at a fixed distance downstream from a junction scour hole (Best, 1988; Ashworth, 1996). Scour holes have also been noted at relatively symmetrical channel confluences in tide-dominated systems, but mid-channel bars are absent because the scoured sediment is exported to marine waters without a compensatory resupply of sediment typical of fluvial systems (Kjerfve *et al.*, 1979; Ginsberg and Perillo, 1999). In contrast to purely fluvial and purely tidal systems, scour holes are absent at junctions between distributaries and tributary blind tidal channels in the Skagit River Delta (personal observation, 2008), while channel bars are present but located at junctions rather than downstream from the junctions. High sediment supply and relatively low sediment export in a prograding delta contribute to channel bar presence and growth in the Skagit Delta, while bidirectional tidal flow may contribute to the symmetrical location of the channel bar/marsh island, upstream and downstream of the blind tributary/delta distributary confluence. The absence of scour holes in Skagit Delta confluences may be explained by the typically extreme asymmetry between the confluent channels. Variations in fluvial confluence bed morphology result from asymmetries in confluence angle, discharge, section-averaged velocity, sediment load, and bed elevation (e.g. Best, 1988; Ashworth, 1996; Boyer *et al.*, 2006). For example, as the tributary/mainstem discharge ratio decreases in fluvial systems, the junction scour depth also decreases (Best, 1988). Delta distributary/blind tidal channel confluences represent an extreme in discharge asymmetry. Skagit distributaries are typically an order of magnitude wider than blind tidal channels, two to three times as deep, have higher ebb tide velocities, and carry more sediment. All of these asymmetries increase during river floods, which travel down the distributaries but not the blind tidal channels.

The depositional meander formation process described for blind tidal channels in the Skagit Delta is a detail of a systemic depositional process of delta progradation that includes distributary elongation, gradient reduction, flow-switching, shoaling, narrowing, and ultimately abandonment and conversion to a blind tidal channel (Hood, 2006). River distributaries have a pervasive and multi-scale influence on delta form and function. Distributary dynamics during delta progradation (mouth bar formation, avulsion, flow-switching, and sediment distribution) are central to large-scale delta development (Coleman, 1988; Berendsen and Stouthamer, 2002; Correggiari *et al.*, 2005; Syvitski *et al.*, 2005; Edmonds and Slingerland, 2007), to meso-scale development of blind tidal channel networks through distributary senescence and abandonment (Hood, 2006), and to relatively fine-scale development of blind tidal channel meanders.

Most numerical and conceptual models of tidal channel development typically assume erosional formation (e.g. Allen, 2000; Fagherazzi and Sun, 2004; D'Alpaos *et al.*, 2005), and they rarely integrate tideflat colonization by marsh vegetation with channel development. However, there are some exceptions. Kirwan and Murray (2007) developed a numerical model integrating tidal marsh accretion and channel development by coupling sediment transport processes with vegetation biomass productivity. Their numerical experiments produced channel development chiefly through depositional processes in the course of marsh progradation, a result consistent with empirical observations of tidal channel development as a consquence of progradation of the Skagit Delta (Hood, 2006). Temmerman *et al.* (2007) developed a numerical model to explain observed tidal channel development in the Westerschelde estuary from the coalescence of patches of vegetation (*Spartina anglica*) colonizing sandbars. These vegetation patches might be considered analogous to the vegetated islands in the Skagit Delta. The Westerschelde model suggests that dense vegetation patches impeded flow through the canopy, thereby forcing flow concentration and channel erosion between patches. Thus, channel formation in this model, although mediated by vegetation patches, was still driven by erosional rather than depositional processes – depositional development of the sandbar platform was not part of the modeling focus. Curiously, marsh accretion never occurred in the model runs. No portion of the initially uniform tideflat platform increased in elevation over the 30-year simulations; there was only channel incision. This result contrasts with the

pattern seen in the Skagit Delta where vegetation colonization clearly results in island elevation gain through accretion, and where the gap between the vegetated island and the adjacent mainland marsh is clearly the tidal channel precursor. Presumably, the contrast between the two systems is due to the stronger progradational character of the Skagit Delta compared to the Westershelde estuary. The numerical models by Kirwan and Murray (2007) and Temmerman *et al.* (2007) illustrate the increasing appreciation of the likely importance of feedbacks between vegetation, hydrodynamics, and sediment transport in the development of marshes and their tidal channels. Interestingly, both models make contradictory predictions of the effects of vegetation density on channel density. Kirwan and Murray (2007) predict a negative correlation, while Temmerman *et al.* (2007) predict a positive one.

Conclusion

Blind tidal channel meander bends can form from primarily depositional rather than erosional processes. Depositional meander formation is likely characteristic of prograding river deltas, particularly during distributary elongation, gradient reduction, flow-switching, and senescence; distributary senescence is characterized by channel shoaling, narrowing, and eventual abandonment. Junctions of tributary blind tidal channels with senescing river distributaries trigger the formation of bars at the tributary mouth which evolve into vegetated marsh islands and force the formation of a tributary meander. This depositional meander formation process is recognizable from diagnostic signatures in channel planform and marsh topography. A sequence of several nearly right-angle tributary meander bends alternating with shore-parallel channel reaches suggests sequential formation of tributary-blocking and meander-forming marsh islands during distributary narrowing. This channel planform is usually accompanied by parallel sequences of marsh ridges and swales that are historical distributary levees adjacent to filled former island/mainland gaps. Marsh islands within delta distributaries are disproportionately associated with blind tidal channel/distributary confluences. Furthermore, blind tidal channel outlet width is positively correlated with the size of the marsh island that forms at the outlet, and the time until island fusion with mainland marsh. These observations suggest confluence hydrodynamics favor sandbar/marsh island development; hydrodynamic modeling of these junctions is likely key to explaining why some channel meanders turn upstream (relative to dominant distributary flow) while others turn downstream – a particularly puzzling question when contrary patterns are observed in adjacent tributary blind tidal channels.

Acknowledgments—Thanks to Tarang Khangaonkar, Guy Gelfenbaum, Matthew Kirwan, and an anonymous reviewer for reviewing the draft manuscript and providing helpful comments.

References

Allen JRL. 2000. Morphodynamics of Holocene salt marshes: a review sketch from the Atlantic and southern North Sea coasts of Europe. *Quaternary Science Reviews* **19**: 1155–1231. DOI. 10.1016/SO277-3791(99)00034-7.

Ashworth PJ. 1996. Mid-channel bar growth and its relationship to local flow strength and direction. *Earth Surface Processes and Landforms* **21**: 103–123.

Babson AL, Kawase M, MacCready P. 2006. Seasonal and interannual variability in the circulation of Puget Sound, Washington: a box model. *Atmosphere-Ocean* **44**: 29–45.

Berendsen HJA, Stouthamer E. 2002. Paleogeographic evolution and avulsion history of the holocene Rhine-Meuse delta, the Netherlands. *Netherlands Journal of Geosciences/Geologie en Mijnbouw* **81**: 97–112.

Best JL. 1988. Sediment transport and bed morphology at river channel confluences. *Sedimentology* **35**: 481–498.

Blondeaux P, Seminara, G. 1985. A unified bar-bend theory of river meanders. *Journal of Fluid Mechanics* **157**: 449–470.

Boyer C, Roy AG, Best JL. 2006. Dynamics of a river channel confluence with discordant beds: flow turbulence, bed load sediment transport, and bed morphology. *Journal of Geophysical Research* **111**: F04007, DOI. 10.1029/2005JF000458

Boyer ME, Harris JO, Turner RE. 1997. Constructed crevasses and land gain in the Mississippi River delta. *Restoration Ecology* **5**: 85–92. DOI. 10.1046/j.1526-100X.1997.09709.x

Coleman JM. 1988. Dynamic changes and processes in the Mississippi River delta. *Geological Society of America Bulletin* **100**: 999–1015.

Correggiari A, Cattaneo A, Trincardi F. 2005. The modern Po Delta system: lobe switching and asymmetric prodelta growth. *Marine Geology* **222–223**: 49–74.

D'Alpaos A, Lanzoni S, Marani M, Fagherazzi S, Rinaldo A. 2005. Tidal network ontogeny: channel initiation and early development. *Journal of Geophysical Research* **110**: FO2001. DOI. 10.1029/2004JF000182

Day Jr JW, Boesch DF, Clairain EJ, Kemp GP, Laska SB, Mitsch WJ, Orth K, Mashriqui H, Reed DJ, Shabman L, Simenstad CA, Streever BJ, Twilley RR, Watson CC, Wells JT, Whigham DF. 2007. Restoration of the Mississippi Delta: lessons from Hurricanes Katrina and Rita. *Science* **315**: 1679–1684. DOI. 10.1126/science. 1137030

Edmonds DA, Slingerland RL. 2007. Mechanics of river mouth bar formation: implications for the morphodynamics of delta distributary networks. *Journal of Geophysical Research* **112**: F02034. DOI. 10.1029/2006JF000574.

Eisma D. 1998. *Intertidal Deposits: River Mouths, Tidal Flats, and Coastal Lagoons*. CRC Press: Boca Raton, FL.

Fagherazzi S, Sun T. 2004. A stochastic model for the formation of channel networks in tidal marshes. *Geophysical Research Letters* **31**: L21503. DOI. 10.1029/2004GL020965

Fagherazzi S, Gabet EJ, Furbish DJ. 2004. The effect of bidirectional flow on tidal channel planforms. *Earth Surface Processes and Landforms* **29**: 295–309. DOI. 10.1002/esp.1016

Fenies H, Faugères J-C. 1998. Facies and geometry of tidal channel-fill deposits (Arcachon Lagoon, SW France). *Marine Geology* **150**: 131–148.

Ginsberg SS, Perillo GME. 1999. Deep-scour holes at tidal channel junctions, Bahia Blanca Estuary, Argentina. *Marine Geology* **160**: 171–182.

Hood WG. 2004. Indirect environmental effects of dikes on estuarine tidal channels: thinking outside of the dike for habitat restoration and monitoring. *Estuaries* **27**: 273–282.

Hood WG. 2006. A conceptual model of depositional, rather than erosional, tidal channel development in the rapidly prograding Skagit River Delta (Washington, USA). *Earth Surface Processes and Landforms*. **31**: 1824–1838. DOI. 10.1002/esp.1381

Hood WG. 2007a. Large woody debris influences vegetation zonation in an oligohaline tidal marsh. *Estuaries & Coasts* **30**: 441–450.

Hood WG. 2007b. Scaling tidal channel geometry with marsh island area: a tool for habitat restoration, linked to channel formation process. *Water Resources Research* **43**: W03409. DOI. 10.1029/2006WR005083

Kirwan ML, Murray AB. 2007. A coupled geomorphic and ecological model of tidal marsh evolution. *Proceedings of the National Academy of Sciences* **104**: 6118–6122.

Kjerfve B, Shao C-C, Stapor Jr FW. 1979. Formation of deep scour holes at the junction of tidal creeks: an hypothesis. *Marine Geology* **33**: M9–M14.

Knighton D. 1984. Fluvial Forms and Processes. Edward Arnold, Ltd: London.

Leopold LB, Wolman MG, Miller JP. 1964. Fluvial Processes in Geomorphology. Dover Publications Inc, New York.

Magnusson A, Hilborn R. 2003. Estuarine influence on survival rates of coho (*Oncorhynchus kisutch*) and Chinook salmon

(*Oncorhynchus tshawytscha*) released from hatcheries on the U.S. Pacific coast. *Estuaries* **26**: 1094–1103.

Marani M, Lanzoni S, Zandolin D. 2002. Tidal meanders. *Water Resources Research* **38**(11): 1225. DOI. 10.1029/2001WR000404

McClennen CE, Housley RA. 2006. Late-Holocene channel meander migration and mudflat accumulation rates, Lagoon of Venice, Italy. *Journal of Coastal Research* **22**: 930–945.

Nickelson TE, Johnson SL. 1991. Survival, contribution, and return of hatchery Coho salmon (*Oncorhynchus kisutch*) released into freshwater, estuarine, and marine environments. *Canadian Journal of Fisheries and Aquatic Sciences* **48**: 248–253.

Reimers PE. 1971. *The Length of Residence of Juvenile Fall Chinook Salmon in Sixes River, Oregon*, Doctoral Thesis, Oregon State University, Corvallis, OR.

Simenstad CA. 1983. *The Ecology of Estuarine Channels of the Pacific Northwest Coast: A Community Profile*, National Coastal Ecosystems Team, Division of Biological Services, Research and Development, Fish and Wildlife Service. US Department of the Interior: Washington, DC.

Solari L, Seminara G, Lanzoni S, Marani M, Rinaldo A. 2002. Sand bars in tidal channels: part 2. Tidal meanders. *Journal of Fluid Mechanics* **451**: 203–238. DOI. 10.1017/S0022112001006565

Syvitski JPM, Kettner A, Correggiari A, Nelson BW. 2005. Distributary channels and their impact on sediment dispersal. *Marine Geology* **222–223**: 75–94.

Syvitski JPM, Saito Y. 2007. Morphodynamics of deltas under the influence of humans. *Global and Planetary Change* **57**: 261–282.

Temmerman S, Bouma TJ, Van de Koppel J, Van der Wal D, De Vries MB, Herman PMJ. 2007. Vegetation causes channel erosion in a tidal landscape. *Geology* **35**: 631–634.

US Federal Register. 1999. *Endangered and Threatened Wildlife and Plants; Listing of Nine Evolutionarily Significant Units of Chinook Salmon, Chum Salmon, Sockeye Salmon, and Steelhead*. US Federal Register **64**(147): 41835–41839.

Wiggins WD, Ruppert GP, Smith RR, Reed LL, Courts ML. 1997. *Water Resources Data, Washington, Water Year 1997*, Water Data Report WA-97-1. US Geological Survey: Tacoma, WA.

Williams GP. 1986. River meanders and channel size. *Journal of Hydrology* **88**: 147–164.

Yang Z, Khangaonkar T. 2009. Modeling tidal circulation and stratification in Skagit River estuary using an unstructured grid ocean model. *Ocean Modelling* **28**: 34–49.

Zar JH. 1999. *Biostatistical Analysis*. Prentice Hall: Englewood Cliffs, NJ.